Garrido Checa, JM.; Medina Folgado, JR. (2012). New neural retwork-derived empirical formulas for estimating wave reflection on Jarlan-type breakwaters. Coastal Engineering. 62:9-18. doi:10.1016/j.coastaleng.2011.12.003.

New neural network-derived empirical formulas for estimating wave reflection on Jarlan-type breakwaters

Joaquín M. Garrido [a] and Josep R. Medina [b]

[a] *Civil Engineer, Iberport Consulting S.A., Parque Empresarial Táctica, C/Botiguers, 3, 46980 Paterna, Spain, jgarrido@iberport.com*

[b] *Professor, Dept. of Transportation, Univ. Politécnica de Valencia, Camino de Vera s/n, 46022 Valencia, Spain, jrmedina@tra.upv.es*

Abstract

A new semi-empirical model is used to estimate the coefficient of reflection for single- and double-perforated chambers in Jarlan-type breakwaters. This semi-empirical model is based on a potential flow theoretical model which was modified with specific, empirical formulas to obtain a much better agreement with the experimental tests. Single-chamber and double-chamber slotted and perforated Jarlan-type breakwaters were tested with 1500 regular wave and 160 random wave runs. Pruned Neural Network models with Evolutionary Strategies were used to identify the nonlinear relationships between the structural and wave climate parameters and the Jarlan-type breakwater reflectivity.

This new semi-empirical model is valid for regular and random waves on single-chamber and double-chamber Jarlan-type breakwaters, providing estimations of the coefficient of reflection with a relative mean squared error lower than 10% for all experimental observations used to calibrate the model.

Keywords: Wave reflection; perforated breakwaters; caisson breakwaters; Jarlan; low reflectivity structures; neural networks.

Article Outline

1. Introduction

The efficiency of any port terminal is usually related to the quay operativity, which depends on vessel characteristics and harbour agitation. Breakwater typologies and harbour layout are the main factors which modify offshore wave conditions within the harbour. Wave reflection on the quays generates multi-reflections which increase harbour agitation and reduce quay operativity and terminal efficiency. These undesired effects can be mitigated by reducing wave reflectivity; therefore, not only are new typologies needed for Low Reflectivity (LR) vertical breakwaters and quaywalls, but research is also necessary to better estimate the wave reflection performance of such structures. Jarlan (1961) was the first to design a breakwater with perforated front wall, a solid back wall and a chamber between the two; this LR breakwater concept is designated as the Jarlan-type breakwater or JTB in the present paper. Experiences in the design and construction of several LR breakwaters have been summarized by Allsop and Bray (1994), Franco (1994), and Takahashi (2006).

The phenomenon of wave reflection on single-chamber JTBs has been studied by different authors using numerical as well as physical experiments. Since the first physical tests carried out by Jarlan (1961) and Marks and Jarlan (1968), and the first analytical model based on acoustic theory (Jarlan, 1965), researchers have analysed the factors affecting wave reflectivity performance of LR breakwaters. Tanimoto and Yoshimoto (1982) investigated experimentally and theoretically analysed the wave reflectivity of partially perforated caissons; Jianyi (1992) tested physical models of multi-chamber LR breakwaters and

showed a significant reduction in wave reflectivity, runup and overtopping. Zhu and Chwang (2001) developed an analytical model to study the wave reflectivity of a slotted front-wall seawall extending from the water surface to a given distance above the seabed. Oumeraci and Kortenhaus (1999) studied experimentally forces and the coefficient of reflection (CR) of LR breakwaters. Takahashi et al. (2002) used volume of fluid (VOF) numerical simulation to evaluate reflection performance of partially-perforated wall caissons for obliquely incident waves. Later Teng et al. (2004) proposed an analytical solution based on the division of the fluid domain for an infinite number of perforated caissons. Suh and Park (1995) developed an analytical model to predict the oblique wave reflection from a fully-perforated wall breakwater mounted on a rubble mound foundation; then Suh et al. (2001 and 2006) extended this model for random waves and a partially-perforated wall caisson.

Other authors have studied the reflection phenomenon in multi-chamber LR breakwaters. Kondo (1979) presented an analytical approach based on long wave theory using regular waves to estimate reflection and transmission coefficients for JTBs having two perforated or slotted walls. Twu and Lin (1991) examined the reflection of a finite number of porous plates. Fugazza and Natale (1992) proposed design formulas valid for regular and irregular waves; this model was based on linear wave theory, calibrated using the results of the experimental measurements reported by Liberatore (1974) and Kondo (1979) for regular waves, and those given by Sawaragi and Iwata (1979) for irregular waves. Williams et al. (2000) modelled the energy dissipation in the chamber fluid region through a damping function. Losada et al. (1993) used the linear

theory for water impinging obliquely on dissipative multilayered media to evaluate the reflection and transmission coefficients. Li et al. (2003) examined the reflection of oblique incident waves with a partially perforated front wall breakwater that consisted of a double-chamber LR breakwater. Kakuno et al. (2003) applied a procedure for design based on the numerical Boundary Integral Method to obtain the coefficient of reflection for double-chamber JTBs. A time-domain method, based on linear velocity potential theory, was presented by Huang (2006) to study the interaction between narrow-banded random waves and LR vertical breakwaters. Liu et al. (2007) examined the reflection of obliquely incident waves by an infinite array of partially-perforated JTBs. Physical experiments of slotted and perforated single- and double-chamber JTBs using regular and random waves were carried out by Garrido and Medina (2006, 2007) to model the nonlinear relationship observed between the coefficient of reflection and the structural and incident wave conditions.

Regarding the influence of reflection in other wave phenomena on vertical breakwaters, Franco and Franco (1999) analysed the results of 2D and 3D experimental model performance of partially-perforated multi-chamber JTBs to establish an overtopping prediction method for regular and random obliquely incident waves. Takahashi et al. (1994), Franco et al. (1998), Bergmann and Oumeraci (2000), Isaacson et al. (2000), Yip and Chwang (2000), Tabet-Aoul and Lambert (2003), Teng et al. (2004), Chen et al. (2007) and Liu et al. (2008) have all conducted studies to calculate the forces on LR vertical breakwaters. Zhu and Zhu (2010) proposed an impedance analytical method to investigate the regular orthogonal wave interaction with the single-chamber JTB and

obtained explicit results for the coefficients of reflection and the wave loads. The conclusions of these studies indicate that both wave forces and overtopping are reduced when wave reflectivity is reduced.

Numerous structural parameters and wave climate variables affect the reflectivity performance of JTBs, making it difficult to study this complex phenomenon and the nonlinear relationships between them. The Neural Network (NN) is a suitable technique to overcome this difficulty. NNs can be considered multi-parametric nonlinear regression methods which are able to capture hidden complex nonlinear relationships between input and output variables. Numerous applications based on NN techniques have been proposed to solve maritime engineering problems; Deo (2010) summarizes past works and explains his experience working with NNs in coastal and ocean engineering. Mase et al. (1995) and Kim and Park (2005) have studied maritime structure designs, especially the design of rouble mound breakwaters, Van Gent and Van den Boogard (1998) examined forces on vertical structures, Panizo and Briganti (2007), the wave transmission behind low-crested breakwaters, and Van Gent et al. (2007) and Verhaeghe et al. (2008), the overtopping prediction of coastal structures.

Pruned NN models optimized with Evolution Strategy (ES) or Simulated Annealing (SA) have also been used to solve maritime engineering problems as they are able to eliminate the experimental noise and to guide the search for simplified empirical models fitted to NN models; for instance, Medina et al. (2002), who used pruned NN models to find empirical formulae to estimate wave overtopping rates. Additionally, Medina (1999) used pruned NN with SA to

analyse runup and overtopping. Medina et al. (2003) also used pruned NNs to study armor damage evolution; Medina and Serrano (2004) for interpolation of time series, and Medina et al. (2006) and Garrido et al. (2010) for wave reflection and transmission. From an initial population of fully-connected NN models, mutation algorithms affecting both NN parameters and topology leading to an optimized pruned NN scheme in which some parameters and sometimes input variables and neurons are eliminated during the ES or SA process.

In the present paper new formulas are given to estimate the CR for single- and double-chamber JTBs. Pruned NN models using ES are employed to identify complex and nonlinear relationships between the structural and wave climate parameters and the breakwater reflectivity. New formulas are given to estimate CR based on results from physical experiments and a modification of the Fugazza and Natale (1992) model. The new formulas are similar to those of the NN model, but explicit and therefore more robust and easier to use than the NN models.

2. Physical experiments

Figure 1 shows the schematic geometry adopted for slotted and perforated single-chamber and double-chamber JTBs.

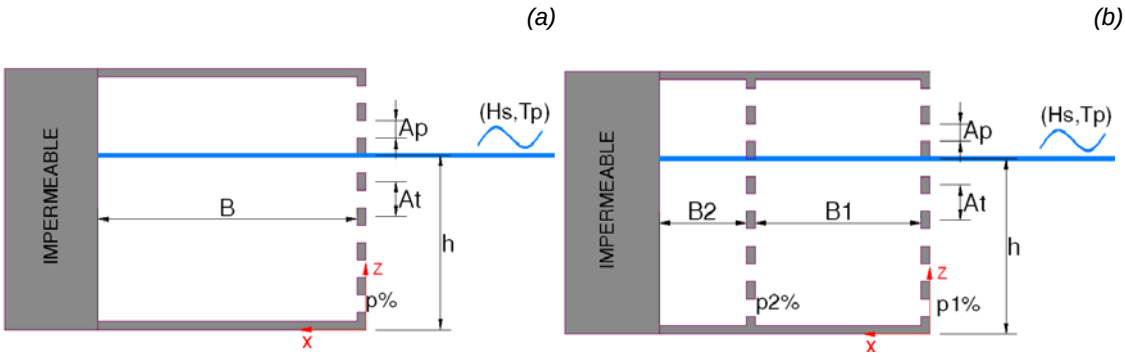

Figure 1. Definition sketch for (a) the single-chamber JTB and (b) the double-chamber JTB.

Physical experiments were conducted at the *Universidad Politécnica de Valencia* (UPV) wave flume (30.0 m x 1.2 m x 1.2 m) to analyse the reflection performance of several single-chamber and double-chamber JTB models. Figure 2 shows the longitudinal cross-section indicating the wave generation area, the transition area with the 4% slope and the model area with the position of the four wave gauges which separated incident and reflected waves.

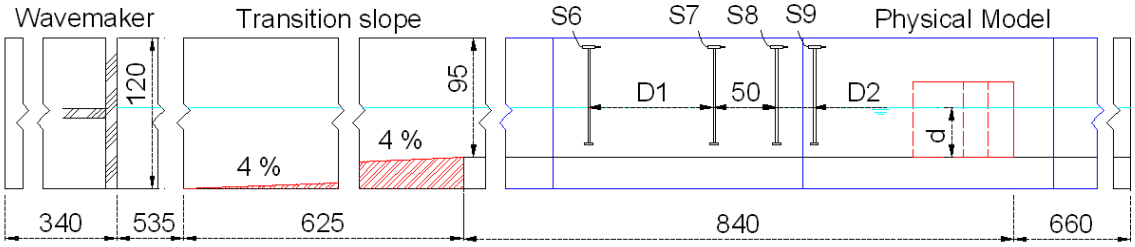

Figure 2. Longitudinal cross section of the UPV wave flume (dimension in cm.).

The number of tests conducted at the UPV wave flume was: 1200 and 80 tests for regular and random waves on slotted walls, and 600 and 80 tests for regular and random waves on perforated walls. During the irregular tests, wave runs of Nw =1000 waves were generated with a JONSWAP (γ=3.3) spectrum, f_{min}=0.5fp and f_{max}=2.5f_p. The wavemaker is a hydraulic piston without an active wave absorption system.

The model was made from 1-cm thick acrylic plates. For each model type, several chamber widths (20<B[cm]<60) were tested with different wall

porosities: 5%<p%<35% for perforated walls with hole diameters being a = 4 cm and a separation of 6<At[cm]<16, and 20%<p%<50% for slotted walls with vertical slits being Ap[cm]=2 and 3 and separation between slits of 6<At[cm]<10 (see Fig. 2). Tests with regular and random waves were done with wave heights of regular wave series in the range of 4<H[cm]<16 and wave periods in the range of 0.6<T[s]<3.5. The random wave series were conducted with significant wave heights ranging from $4<H_s[cm]<15$ and a peak period ranging from $1.0<T_p[s]<2.5$. Experiments were carried out at a water depth in the range 0.24<h[m]<0.5.

The incident and reflected waves were analysed using the time-domain LASA method (Medina, 2001), which is able to separate nonlinear incident and reflected waves in time domain with nonstationary conditions, allowing for the non-application of the reflection absorption system of the wavemaker. The CR is defined as the ratio between the reflected and incident wave heights for regular waves and the ratio between reflected and incident significant wave heights for random waves, using four wave gauges (S6, S7, S8 and S9) and measured in the S8 wave gauge position (see Fig. 2).

Experiments were carried out considering different porosities for perforated walls (Fig. 3a) and slotted walls (Fig. 3b). Slotted and perforated walls show a similar CR for a similar porosity, and a minimum CR was obtained when porosity ranged 20%<p%<30%. Single-chamber JTB models showed a CR less than 60% in the range of 0.1<B/L<0.3. Porosity is defined as the ratio between the open area, slotted or perforated, and total area, $p\%=100*A_p/A_t$.

(a) *(b)*

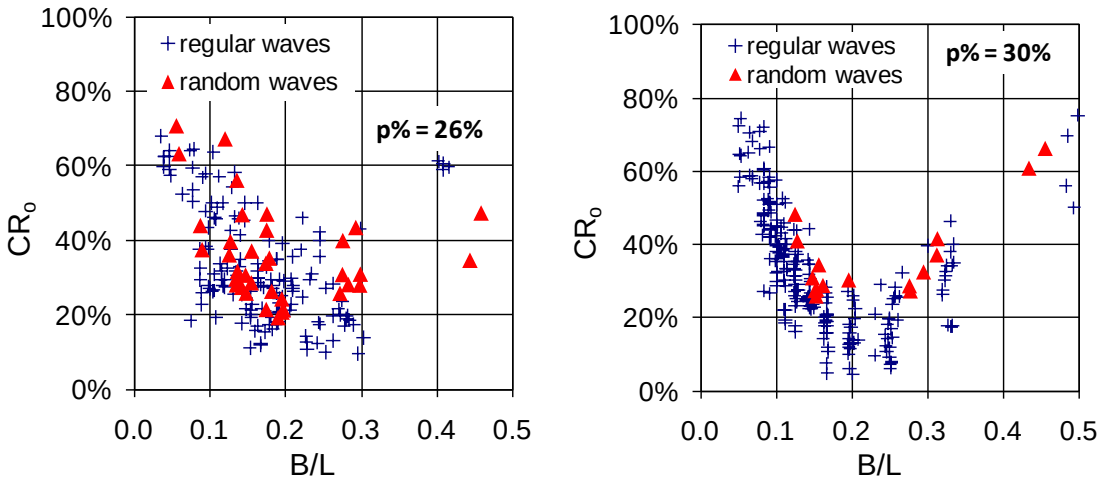

Figure 3. Measured CR for (a) perforated single-chamber JTBs and (b) slotted single-chamber JTBs.

Experimental tests of double-chamber JTBs do not show the relationship between CR and B/L which typically corresponds to single-chamber JTBs. For double-chamber JTBs, the CR showed a lower value in a wider range of B/L. For values of B/L greater than 0.35, multiple-chamber JTBs are better at reducing the wave reflection than single-chamber JTBs. Figure 4 shows the results corresponding to double-chamber JTBs.

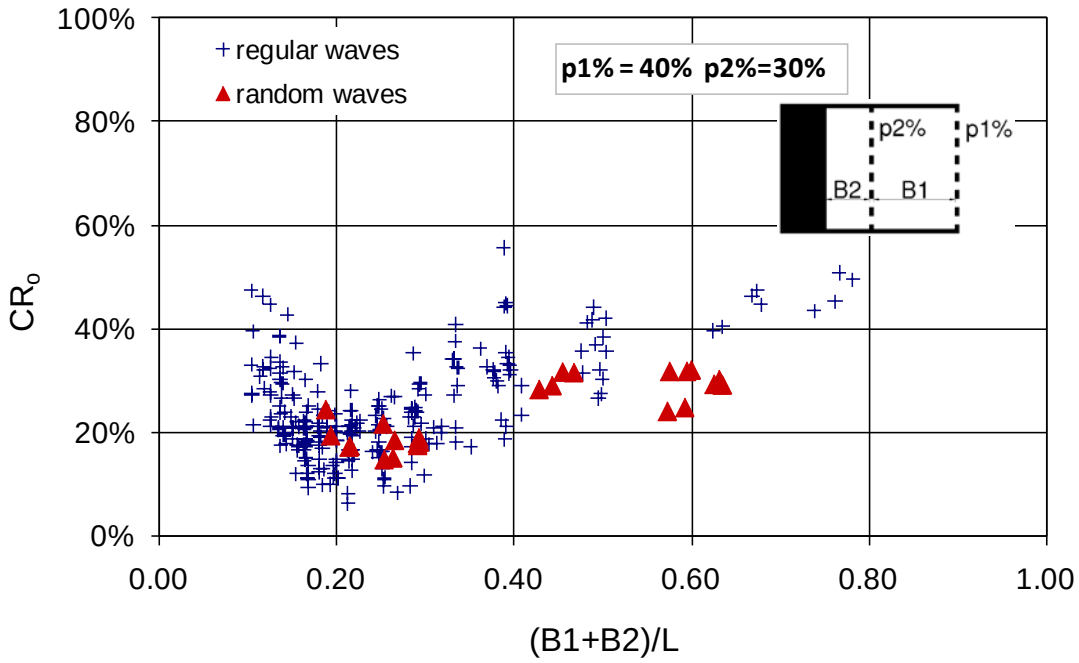

Figure 4. Measured CR for slotted double-chamber JTBs.

3. Analytical model

Most analytical models developed to estimate CR of JTBs are based on linear theory. The velocity potentials for reflected and transmitted waves are determined by applying the matching conditions at the wall boundary and the far field boundary conditions. The Fugazza and Natale (1992) model, noted as the FN0 model, is taken in this paper as representative of analytical models for JTBs. The FN0 model was improved with the model proposed by Williams et al. (2000), noted as the W0 model, incorporating the concept of energy dissipation within the chamber, and modelled empirically by a damping function. Both FN0 and W0 models lead to a closed-form solution for the CR for multi-chamber JTBs. These methods assume regular, long-crested and small-amplitude waves, normally incident on the structure. The FN0 and W0 models are described in Appendices A and B, respectively.

3.1. FN0 and W0 models

FN0 and W0 models are based on potential flow theory, which considers that the fluid is incompressible, non-viscous and irrotational. The basic phenomena governing the wave-structure interaction can be separated in three groups: (1) inertial effects, (2) resistance, and (3) wave energy damping. The inertial effects are considered by the β function, expressed as [A.6], related to phase shift between velocity and pressure on either side of the perforated wall. The resistance is caused by reflection and wave transmission through the perforated wall, which depends on the geometry of the wall, material characteristics and the wall porosity, p%. The energy dissipation within the chambers, which is considered as a damping phenomenon for the W0 model, is expressed as [B.1] in Appendix B.

In the FN0 model, the inertial effects depend on the plate orifice coefficient, α, given by Equation [A.7] in Appendix A, which in turn depends on the empirical discharge coefficient, C_C, and the geometry of the perforated wall.

For single-chamber JTBs, the FN0 was originally calibrated with experimental results using regular waves with wall porosities p%=20%, 33% and 50%. For double-chamber JTBs, the FN0 model was calibrated with p1%=33%, p2%=20%, p1%=33%, p2%=65% and p1%=20%, p2%=20%, as given by Liberatore (1974) and Kondo (1979). For random waves, the FN0 model was calibrated with the data reported by Sawaragi and Iwata (1979). As a result of the calibration process of the FN0 model, Cc was set to Cc= 0.55 used in [A.7].

For single-chamber JTBs, the W0 model was originally calibrated with experimental results having p%=34% and 42%. For double-chamber JTBs

p1%=38% and p2%=20%, as given by Kondo (1979) and Two and Lin (1991), were used. The W0 model used the same value Cc=0.55 as that used for the FN0 model. The coefficient of reflection estimated by the W0 model for single- and double-chamber JTBs is expressed by [B.2] and [B.3] in Appendix B, respectively.

3.2. Validation of FN0 and W0 models

The FN0 and W0 models were compared with the experimental results obtained at the UPV wave flume for single- and double-chamber JTBs, in which different porosities, for both regular waves and random waves, were tested. The relative Mean Squared Error (MSE), r_{MSE}, was used to measure the goodness of fit of the different models to the estimated CR, according to equation [1].

$$r_{MSE} = \frac{\sum_{j=1}^{N} \left(CR_e - CR_o \right)_j^2}{\sum_{j=1}^{N} \left(CR_o^2 \right)_j} \qquad [1]$$

in which $(CR_e)_j$ is the estimated reflection coefficient of test j, and $(CR_o)_j$ is the observed reflection coefficient of test j.

For single-chamber JTBs, columns 2, 3, 6 and 7 in Table 1 show the r_{MSE} of the estimated CR using the FN0 and W0 models with regular and random waves. For double-chamber JTBs, columns 3, 4, 7 and 8 in Table 2 show the r_{MSE} of the estimated CR using the FN0 and W0 models, with regular and random waves. Fig. 5 compares estimated and measured CR of the FN0 model with experimental results for one case using regular waves and random waves.

p%	regular waves				random waves			
	CR_{FN0}	CR_{W0}	CR_{FN1}	CR_{W1}	CR_{FN0}	CR_{W0}	CR_{FN1}	CR_{W1}
(1)	(2)	(3)	(4)	(5)	(6)	(7)	(8)	(9)
13%	14.0%	14.2%	5.2%	4.8%	24.5%	24.8%	1.8%	1.8%
20%	14.3%	14.5%	8.3%	7.8%	6.7%	6.9%	3.5%	3.6%
26%	16.8%	13.7%	16.5%	14.8%	8.9%	8.1%	9.0%	8.1%
30%	14.3%	15.2%	14.5%	13.7%	8.9%	7.0%	8.7%	6.9%
40%	8.2%	8.9%	6.4%	5.7%	17.2%	13.0%	14.0%	10.5%
50%	4.1%	3.4%	4.7%	4.5%	19.5%	20.4%	24.5%	25.1%
Mean	11.9%	11.7%	9.3%	8.6%	14.3%	13.4%	10.2%	9.3%

Table 1. r_{MSE} of CR for single-chamber JTBs.

p1%	p2%	regular waves				random waves			
		CR_{FN0}	CR_{W0}	CR_{FN1}	CR_{W1}	CR_{FN0}	CR_{W0}	CR_{FN1}	CR_{W1}
(1)	(2)	(3)	(4)	(5)	(6)	(7)	(8)	(9)	(10)
13%	5%	23.5%	23.3%	4.1%	3.1%	26.0%	24.3%	2.2%	1.8%
30%	20%	32.8%	50.8%	31.8%	27.1%	5.7%	11.8%	6.0%	12.6%
40%	30%	14.9%	99.5%	17.7%	30.5%	4.8%	42.6%	5.0%	33.0%
Mean		23.7%	57.9%	17.8%	20.3%	12.1%	26.2%	4.4%	15.8%

Table 2. r_{MSE} of CR for double-chamber JTBs.

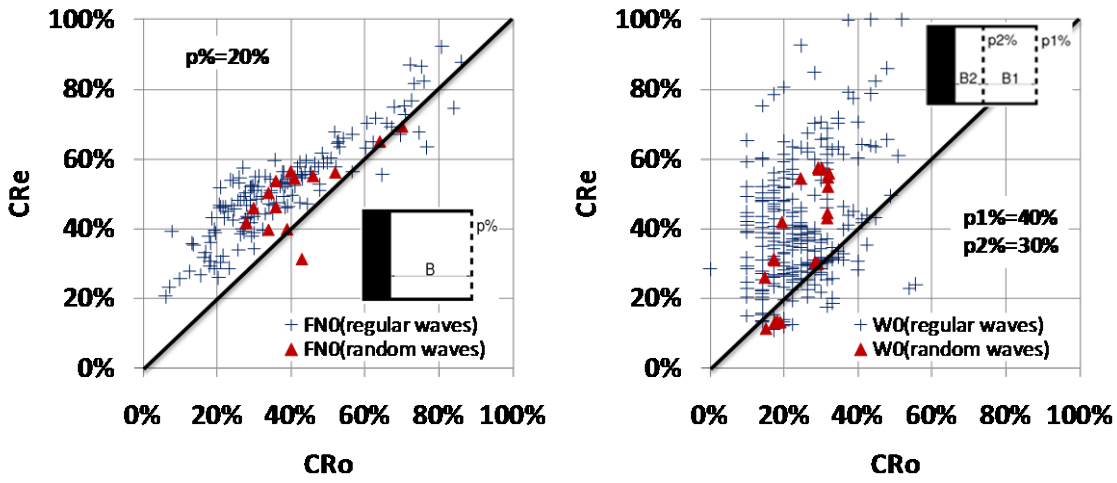

Figure 5. Comparison of observed and estimated reflected energy for the FN0 model.

The r_{MSE} given for single-chamber JTBs in Table 1 indicates the W0 model is only slightly better than the FN0 model, both for regular and random waves; however, the r_{MSE} for double-chamber JTBs given in Table 2 indicates that the

FN0 model is significantly better than the W0 model both for regular and random waves.

The plate orifice coefficient, α, given by expression [A.7] in Appendix A, only depends on the porosity; therefore, a better estimate of the CR is possible if this empirical parameter is modified.

The results obtained by the FN0 model, with different Cc coefficients, are compared with experimental results of single-chamber JTBs in the case of regular waves to obtain the best fit for Eq. [1] for different porosities. Thus, the plate orifice coefficient was empirically modified.

$$\alpha = -44\ln(p) - 16 \qquad [2]$$

Eq. [2] was used to modify the FN0 and W0 models to obtain new models referred to as FN1 and W1, respectively. For single-chamber JTBs, columns 4, 5, 8 and 9 in Table 1 show the r_{MSE} of the estimated CR using the FN1 and W1 models with regular and random waves. For double-chamber JTBs, columns 5, 6, 9 and 10 in Table 2 show the r_{MSE} of the estimated CR using the FN1 and W1 models with regular and random waves.

The r_{MSE} given by both the FN1 and W1 models is better than that obtained with the FN0 and W0 models for most porosities. The W1 model is worse than the FN1 model for double-chamber JTBs using random waves. Therefore, the W1 model is not considered for further improvement in this study.

The FN1 model is better than the FN0, W0 and W1 models but, in order to improve the FN1 model, a pruned NN model using ES will serve as an auxiliary tool to find a new model to estimate the CR of single- and double-chamber JTBs, as the pruned NN model is able to consider nonlinear relationships

between the variables involved in the phenomenon, which are not taken into account in the model FN1.

4. Neural Network models

4.1. Pruned Neural Network (NN) models by Evolution Strategy (ES)

NNs are inspired in the functioning of the nervous system of animals and use concepts such as neurons, axon and synaptic junctions, in which the input-output relationship is captured by the NN model. NNs can be considered multi-parametric nonlinear regression methods which are able to capture hidden complex nonlinear relationships between input and output variables.

Numerous applications based on backpropagation learning algorithms have been proposed to solve maritime engineering problems. Fully connected NN models trained with backpropagation algorithms and pruned NN models optimized with ES have also been used to solve a variety of water engineering applications. In this paper, NN models optimized with ES are used to discover the nonlinear relationships between CR and the structural and wave climate variables. From an initial population of fully-connected NN models, mutation algorithms affecting both NN parameters and topology lead to an optimized pruned NN scheme in which some parameters and sometimes input variables and neurons are eliminated during the evolutionary process. The best NN models survive in an environment where the generalized NN error is measured using the Predicted Squared Error (PSE) given by Moody (1992), $PSE=MSE[1+2P/(N-P)]$, in which MSE is the mean squared error; P is the number of free parameters, and N is the number of cases used for training. The best NN models not only agree well with training observations but they also

have a minimum number of parameters, including the elimination of input variables which are not relevant in explaining the output.

The wave attack variables considered to optimize regular waves are H_i = incident wave height and L_i=wave length corresponding to incident wave period, T_i, while for random waves, $H_{mo,i}$ = incident significant wave height and $L_{01,i}$= wave length corresponding to the incident wave period, $T_{01,i}$. The structural variables considered in this study for single-chamber JTBs are: B=chamber width; p%= porosity and h=water depth. For double-chamber JTBs, B1 and B2 are frontal and rear chamber widths, and p1 and p2 are porosities of frontal and rear perforated walls, respectively. Fig. 2 illuestrates the single- and double-chamber JTBs.

The use of relevant dimensionless variables facilitate the optimisation process of the NN models; however, ES is able to select the most significant variables. The following dimensionless variables commonly used in maritime engineering practice were taken as inputs for single-chamber JTBs: B/L, H/L, H/h and $p\%=100\cdot A_p/A_t$. For double-chamber JTBs, the following dimensionless variables were used: B1/L, (B1+B2)/L, B1/(B1+B2), H/L, H/h, p1, p2, p1/p2. In addition to the structural variables and wave climate variables, the CR estimation of the FN1 model was taken as an additional input, noted as CR_{FN1}, which allows for the consideration of the result of the improved analytical FN1 model. The experimental tests were randomly separated in three groups: 80% for training, 10% for validation and 10% for testing, for regular and random waves.

4.2. NN simulation and modified FN1 model

The ESs have proved to be very effective to optimize both the topology and parameters of pruned NN models. Evolutionary processes of both NN models for single- and double-chamber JTBs eliminated all except two input variables: RE_{FN1} and p% for single-chamber JTBs and RE_{FN1} and p2% for double-chamber JTBs. This result facilitates the process of finding the relationships captured by the NN models, because this process is more difficult when the number of significant input variables is higher. The NN estimations are valid for single- and double-chamber JTBs within the ranges specified in Table 3.

	B/L	H/L	H/h	p1%	p2%
single-chamber JTBs	1/20-1/2	1/150-1/10	1/15-1/3	13%-50%	-
double-chamber JTBs	1/10-1	3/1000-1/10	1/250-1/2	13%-35%	5%-30%

Table 3. Range of regular wave variables

NN models are usually black boxes for the users. In order to make explicit the nonlinear relationships captured by the NN models, multiple simulations of synthetic tests from the input variables classified by the pruned NN model were performed within the range of the data given in Table 3. Figs. 6a and 6b show the CR_e in single- and double-chamber JTBs, respectively, obtained through the simulations of synthetic tests for regular waves.

(a) (b)

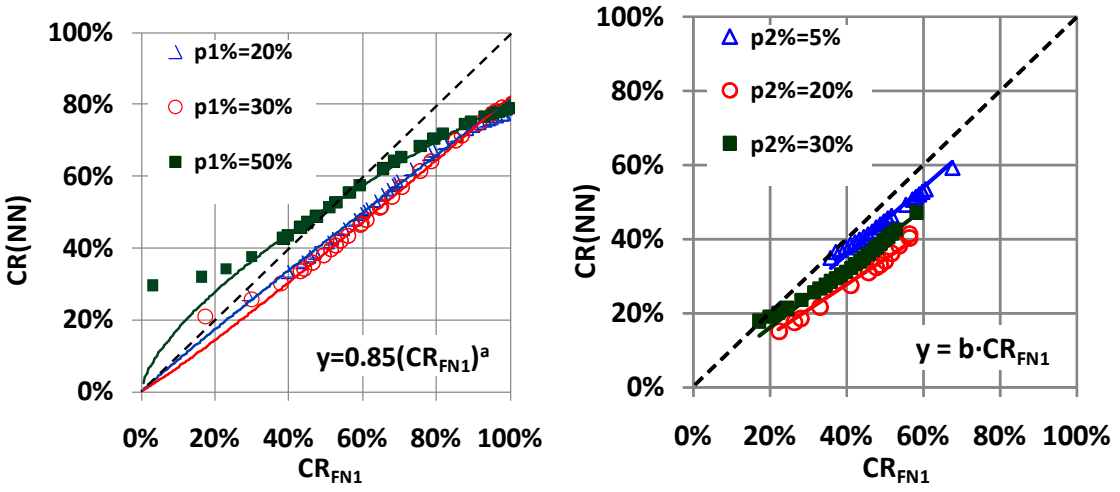

Figure 6. Fitting lines for CR(NN) related to CR_{FN1} for: (a) single-chamber JTBs and (b) double-chamber JTBs.

The fitting lines shown in Fig. 6 are the function $y=0.85\cdot(CR_{FN1})^a$ for single-chamber JTBs and the function $y=b\cdot CR_{FN1}$ for double-chamber JTBs, where parameters "*a*" and *"b"* are quadratic functions depending on wall porosity, p% and p2%, respectively, obtained from the fit of both functions for different values of porosity and CR_{FN1} from the analysis of NN simulations. The following formula was obtained for single-chamber JTBs (regular waves):

$$CR(regular) = 0.85\left(CR_{FN1}\right)^{-12\,p^2+6.7\,p+0.2} \qquad [3]$$

where p is the wall porosity of the single-chamber JTBs, and CR_{FN1} is the reflected energy estimated by the FN1 model.

The formula for double-chamber JTBs (regular waves) was:

$$CR(regular) = \left(\frac{28}{3}\,p_2^2 - \frac{11}{3}\,p_2 + 1\right)\cdot CR_{FN1} \qquad [4]$$

where p_2 is the porosity of the rear perforated wall for double-chamber JTBs, and CR_{FN1} is the coefficient of reflection estimated by the FN1 model and CR(regular) is the coefficient of reflection estimated by the new formula, which is valid for regular waves on JTBs and the ranges given in Table 3.

For random waves, both single- and double-chamber JTBs satisfy

$$CR(random) = 0.8 \cdot CR(regular) + 0.1 \quad [5]$$

where CR(random) is the coefficient of reflection estimated by the new formula, which is valid for random waves on JTBs and the ranges given in Table 4.

	B/L_{01}	Hs/L_{01}	Hs/h	p1%	p2%
single-chamber JTBs	1/20-1/2	1/100-1/10	1/10-1/3	13%-50%	-
double-chamber JTBs	1/7-2/3	1/100-3/50	1/8-1/3	13%-40%	5%-30%

Table 4. Range of random wave variables

The r_{MSE} of CR(regular) given by Eqs. [3] and [4] and of CR(random) given by Eq. [5] is shown in Tables 5 and 6 for single- and double-chamber JTBs, respectively.

p%	$CR(NN_{FN1})$	$CR(NN_{W1})$	**CR(regular)**	$CR(NN_{FN1})$	$CR(NN_{W1})$	**CR(random)**
13%	2.9%	3.1%	3.5%	1.3%	1.3%	1.3%
20%	3.4%	4.0%	2.8%	0.8%	0.9%	3.1%
26%	9.7%	9.4%	10.7%	7.3%	7.2%	7.1%
30%	5.5%	5.5%	5.7%	3.4%	3.4%	3.6%
40%	3.1%	2.8%	3.3%	7.4%	7.3%	2.8%
50%	1.9%	1.9%	2.6%	0.7%	0.8%	3.0%
Mean	4.4%	4.4%	4.8%	3.5%	3.5%	3.5%

Table 5.- r_{MSE} of CR for single-chamber JTBs.

p1%	p2%	$CR(NN_{FN1})$	$CR(NN_{W1})$	**CR (regular)**	$CR(NN_{FN1})$	$CR(NN_{W1})$	**CR(random)**
13%	5%	1.0%	1.1%	2.0%	0.3%	0.4%	0.3%
30%	20%	5.8%	7.4%	5.6%	1.3%	1.5%	1.0%
40%	30%	8.1%	11.8%	8.2%	1.4%	7.2%	1.1%
Mean		5.0%	6.8%	5.3%	0.9%	2.7%	0.8%

Table 6. r_{MSE} of CR for double-chamber JTBs.

The coefficient of reflection estimated by NN models is specified as CR_{NN}, while CR(regular) and CR(random) are the coefficients of reflection estimated by Eqs. [3] to [5].

The new formulas are similar to that of the NN model, but Equations [3] to [5] are explicit and therefore more robust and easier to use than the NN models. Pruned NN models using ESs were applied here to identify complex and non-linear relationships among different variables affecting the reflection phenomena on JTBs.

5. Comparison with other authors

To examine the effectiveness of the present model in comparison to the models proposed by other authors, the predictions of the coefficient of reflection for JTBs given by the present model is compared with other models and validated with data reported by other authors.

Zhu and Zhu (2010) compared the theoretical predictions of their impedance analytical method with those obtained experimentally by Two and Lin (1991), Kondo (1979) and Seyama and Kiyosi (1978). Kondo (1979) carried out a series of experiments with regular waves on single- and double chamber JTBs; B[m]=0.25 for single-chamber JTBs, and B1[m]=B2[m]=0.25 for double-chamber JTBs. H[cm]=4 was tested and the wave period was between 5<T[s]<12. The perforated walls were made of 6mm-thick steel plate, the holes measured 20 mm in diameter and the tested porosities were p%=20% and p%=34%.

Two and Lin (1991) also carried out a series of regular wave experiments on single- and double-chamber JTBs. Wave heights were 2<H[cm]<4; wave

periods were 0.85<T[s]<3 and the water depth was h[m]=0.5. The chamber width was B[m]=0.44 for single-chamber JTBs and B1[m]=B2[m]=0.44 for double-chamber JTBs. The perforated walls were made of four 1 mm-thick steel plates, the holes were 6 mm in diameter and the porosity was p%=44%.

Zhu and Chwang (2001) experimented with regular waves normally incident upon a single-chamber JTB to verify the results of their analytical model. Wave height was H[cm]=3; wave periods were 0.7<T[s]<1.0 and water depth h[m]=0.32. The chamber width was between 0.024<B[m]<0.484 and the slotted seawall has a porosity of p%=20%.

Table 7 shows the range of variables for regular waves and the different number of chambers (Nc), as well as the number of experimental tests (Nt), the perforated typology (PT), either PW = perforated walls or SW = slotted walls. r_{MSE} is the relative MSE of the models given by Eq. 1. Figure 7 compares observed and estimated coefficients of reflection for regular waves.

									Model (year)- r_{MSE}		
Regular waves	**Nc**	**PT**	**Nt**	**B/L**	**H/L**	**H/h**	**p1%**	**p2%**	**FN0 (1992)**	**Zhu & Zhu (2010)**	**Present**
Kondo(1979)	1	PW	9	1/9-1/2	1/57-1/10	1/25	20%	-	14.1%	23.3%	5.8%
	2	PW	18	1/8-1/1.5	1/156-1/29	1/25	20% & 34%	20%	16.4%	-	6.0%
Two and Lin (1991)	1	PW	30	1/18-1/3	1/400-1/28	1/25-2/25	44%	-	12.7%	0.6%	4.4%
	2	PW	30	1/10-1/1.3	1/400-1/28	1/25-2/25	44%	44%	50.2%	-	5.2%
Zhu and Chwang (2001)	1	SW	25	1/65-1/2	1/52-1/26	1/11	20%	-	1.3%	4.8%	1.9%
This paper	1	PW	358	1/20-1/2	1/150-1/10	1/15-1/3	13%-35%	-	14.5%	8.3%	7.8%
	1	SW	605				20%-50%	-	10.6%	17.0%	3.7%
	2	PW	212	1/10-1	3/1000-1/10	1/250-1/2	13%-35%	5%-26%	21.9%	-	2.4%
	2	SW	382				30%-40%	20%-30%	20.6%	-	7.6%

Table 7. Comparison of different models and experimental test results (regular waves).

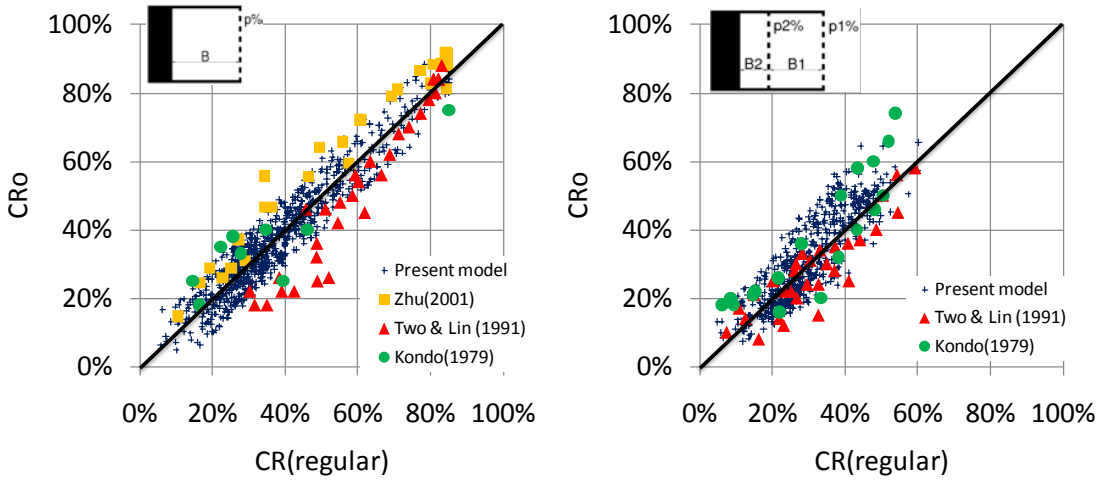

Figure 7. Comparison of different models and experimental test results (regular waves).

Suh et al. (2001) carried out experiments on random waves normally incident upon a single-chamber JTB. Chamber widths were B[m]=0.15, 0.30, 0.45 and 0.60 Laboratory experiments were conducted to examine the reflection of irregular waves for p%=33%. Wave heights were 3<Hs[cm]<10; wave periods were 1.0<Ts[s]<2.0 and the water depth was h[m]=0.5 m during the tests. Sawaragi and Iwata (1979) conducted experimental tests to examine the reflection of irregular waves for single-chamber JTBs with chamber widths in the range of 0.10<B[m]<0.82 and p%=50%. The wave heights were H[cm]=2, wave periods Ts[s]=0.7 and water depth h[m]=0.25.

Table 8 shows the range of variables for random wave tests depending on the number of chambers (Nc), number of experimental tests (Nt) and r_{MSE}. Figure 8 compares observed and estimated coefficients of reflection for random waves.

									Model(year) - r_{MSE}	
Random waves	**Nc**	**PT**	**Nt**	**B/L_{01}**	**Hs/L01**	**Hs/h**	**p1%**	**p2%**	**FN0(1992)**	**Present**
Sawaragi & Iwata (1979)	1	PW	8	1/7-1/0.85	1/34-1/34	1/12-1/12	50%	-	18.1%	10.4%
Suh et al. (2001)	1	SW	60	1/3-1/25	1/125-1/25	1/14-1/4	33%	-	9.7%	13.3%
This paper	1	PW	60	1/20-1/2	1/100-1/10	1/10-1/3	13%-50%	-	13.8%	5.8%
	1	SW	58	1/20-1/2	1/100-1/10	1/10-1/3	13%-50%	-	12.4%	3.2%
	2	PW	21	1/7-2/3	1/100-3/50	1/8-1/3	13%-35%	5%-26%	23.6%	1.6%
	2	SW	32				30%-40%	20%-30%	5.1%	1.1%

Table 8.- Comparison of different models and experimental test results (random waves).

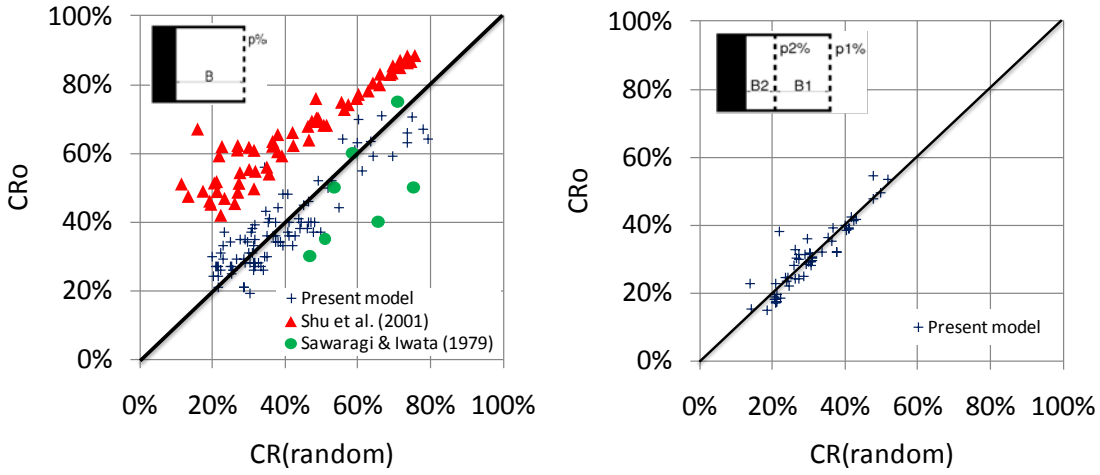

Figure 8.- Comparison of different models and experimental test results (random waves).

The present model is the best when compared to other data and models reported in literature. Only the results of Suh et al. (2001) for single-chamber JTBs and random waves are slightly better than the newly proposed model; however, one should take into consideration that different authors have used slightly different experimental methodologies (wave analysis techniques, experimental set up, etc.).

6. Conclusions

Based on more than 1500 regular wave tests and 160 random wave tests carried out in the UPV wave flume, the plate orifice coefficient, α, of FN0 and W0 models was modified for single- and double-chamber JTBs to obtain FN1

and W1 models. This empirical modification of the inertial term improved the agreement with experimental observations for both FN0 and W0 models. However, the disagreement between certain experimental observations and CR estimations by the FN1 and W1 models show r_{MSE}>20%.

Pruned NN models with ES were used to identify an explicit empirical modification of the FN1 model for a better agreement with the experimental data. The ESs have proved to be very effective optimizing both the topology and parameters of pruned NN models, facilitating the process of finding the relationships captured by the NN models. Thus, the new formulas are similar to those of the NN model, but the obtained equations are explicit and therefore more robust and easier to use than the NN models.

Numerical simulations and graphic representations facilitated the search for simple empirical equations to modify FN1. As a result, an empirical relationship between wall porosities and CR was found to significantly improve the FN1 model. The formulas given in Eqs. [3] to [5], significantly improved the goodness of fit to the experimental observations given by FN1 model. The new semi-empirical model provides an estimation of the coefficient of reflection with a low relative MSE; r_{MSE}< 8% for regular wave tests and r_{MSE}< 6% for random wave tests. When compared with experimental data given by other authors, errors were similar for regular wave tests and slightly higher (r_{MSE}< 13.5%) for random wave tests. Therefore, it can be stated that this semi-empirical model provides good estimations for single- and double-chamber JTBs under regular as well as random waves.

7. Acknowledgments

This research was funded by the Spanish Ministry of Science and Innovation and FEDER (grants TRA2006-11114/TMAR and CADIMA-P11/08). The authors thank Debra Westall for revising the manuscript as well as the reviewers for their comments and suggestions which have enhanced the quality of the paper.

8. References

Allsop, N.W.H., Bray, R.N., 1994. Vertical breakwaters in the United Kingdom: historical and recent experience. Proceedings of the International Workshop on Wave Barriers in Deepwaters, Port and Harbour Research Institute, pp. 76–128.

Bergmann, H., Oumeraci, H., 2000. Wave loads on perforated caisson breakwaters. Proceedings of the 27th International Conference on Coastal Engineering, ASCE, pp. 1622-1635.

Chen, X.F., Li, Y.C., Teng, B., 2007. Numerical and simplified methods for the calculation of the total horizontal wave force on a perforated caisson with a top cover. Coastal Engineering, 54, pp. 67–75.

Deo, M.C., 2010. Artificial neural networks in coastal and ocean engineering. Indian Journal of Marine Science, 39(4), pp. 589-596.

Franco, L., 1994. Vertical breakwaters: the Italian experience. Coastal Engineering, 22, pp. 31-55.

Franco, L., de Gerloni, M., Passoni, G., Zacconi, D., 1998. Wave forces on solid and perforated caisson breakwaters: comparison of field and laboratory

measurements. Proceedings of the 26th International Conference on Coastal Engineering, ASCE, pp. 1945–1958.

Franco, C., Franco, L., 1999. Overtopping Formulas for Caisson Breakwaters with Nonbreaking 3D Waves. Journal of Waterway, Port, Coastal and Ocean Engineering, ASCE, 125(2), pp. 98-108.

Fugazza, M., Natale, L., 1992. Hydraulic performance of perforated breakwater. Journal of Waterway, Port, Coastal and Ocean Engineering, ASCE, 118(1), pp. 1–14.

Garrido, J.M., Medina, J.R., 2006. Study of reflection of perforated vertical breakwaters. Proceedings of the 30th International Conference on Coastal Engineering, ASCE, pp. 4325–4336.

Garrido, J.M., Medina, J.R., 2007. Modelo neuronal para estimar la reflexión del oleaje en diques verticales antirreflejantes. Libro de Ponencias de las IX Jornadas españolas de Costas y Puertos, AZTI-Tecnalia, pp. 486-495 (in Spanish).

Garrido, J.M., Ponce de León, D., Berruguete, A., Martínez, S., Manuel, J., Fort, L., Yagüe, D., González-Escrivá, J.A., Medina, J.R., 2010. Study of reflection of new low-reflectivity quay wall caissons. Proceedings of the 32nd International Conference on Coastal Engineering, ASCE. Paper No. 213 / structures.27.

Huang, Z.H., 2006. A method to study interactions between narrow-banded random waves and multi-chamber perforated structures. Acta Mechanica Sinica, 22 (4), pp. 285–292.

Isaacson, M., Baldwin, J., Allyn, N., Cowdell, S., 2000. Wave interactions with perforated breakwater. Journal of Waterway, Port, Coastal, and Ocean Engineering, ASCE,126 (5), pp. 229–235.

Jarlan, G.E., 1961. A perforated vertical breakwater. The Dock and Harbour Authority, Vol. 41, No. 486, pp. 394-398.

Jarlan, G.E., 1965. The application of acoustic theory to the reflective properties of coastal engineering structures. Quart. Bulletin, National Research Council Canada, pp. 23-64.

Jianyi, W., 1992. Experimental study of perforated caisson breakwaters. China Ocean Engineering, Vol. 6, pp. 65-78.

Kakuno, S., Tsujimoto, G., Shiozaki, Y., 2003. A design method for double slit-wall breakwaters. Proceedings of Coastal Structures 2003, ASCE, pp. 295-304.

Kim, D.H., Park, W.S., 2005. Neural Network for Design and Reliability Analysis of Rouble Mound Breakwaters. Ocean Engineering, 32(11-12), pp. 1332-1349.

Kondo, H., 1979. Analysis of breakwaters having two porous walls. Proceedings of Coastal Structures 1979, ASCE, pp. 962-977.

Li, Y.C., Dong, G.H., Liu, H.J., Sun, D.P., 2003. The reflection of oblique incident waves by breakwaters with double-layered perforated walls. Coastal Engineering, 50, pp. 47–60.

Liberatore, L., 1974. Experimental investigation on wave-induced forces on Jarlan-type perforated breakwaters. Atti. del XIV Convegno di Idraulica e Costruzioni Idrauliche, Napoli, Italy, pp. 101-109.

Liu, Y., Li, Y.C., Teng, B., 2007. The reflection of oblique waves by an infinite number of partially perforated caissons. Ocean Engineering, 34, pp. 1965–1976.

Liu, Y., Li, Y., Teng, B., Jiang, J., Ma, B., 2008. Total horizontal and vertical forces of irregular waves on partially perforated caisson breakwaters. Coastal Engineering, 55, pp. 537–552.

Losada, I.J., Losada, M.A., Baquerizo, A., 1993. An analytical method to evaluate the efficiency of porous screens as wave dampers. Applied Ocean Research, 15, pp. 207–215.

Marks, W., Jarlan, G.E., 1968. Experimental studies on fixed perforated breakwater. Coastal Engineering, 68, pp. 121-1140.

Mase, H., Sakamoto, M., Sakai, T., 1995. Neural Network for Stability of Rouble Mound Breakwaters. Journal of Waterways, Port, Coastal and Ocean Engineering Division, 121(6), pp. 294-299.

Medina, J.R., 1999. Neural Network Modelling of Runup and Overtopping. Proceedings of Coastal Structures 1999, A.A. Balkema, Vol. 1, pp. 421-429.

Medina, J.R., 2001. Estimation of incident and reflected waves using simulated annealing. Journal of Waterway, Port, Coastal and Ocean Engineering, 127(4), pp. 213-221.

Medina, J.R., González-Escrivá, J.A., Garrido, J.M., De Rouck, J., 2002. Overtopping analysis using neural networks. Proceedings of the 28th International Conference on Coastal Engineering, ASCE, pp. 2165-2177.

Medina, J.R., Garrido, J.M., Gómez-Martín, M.E., Vidal, C., 2003. Armor Damage Analysis using Neural Networks. Proceeding of Coastal Structures 2003, ASCE, pp. 236-246.

Medina, J.R., Serrano-Hidalgo, O., 2004. Interpolation of Time Series of Sea State Variables using Neural Networks. Proceedings of the 29th International Conference on Coastal Engineering, ASCE, Vol. 1, pp. 985-996.

Medina, J.R., Muñoz, J.J., Gómez-Pina, G., 2006. Transmission and Reflection of Modular Detached Breakwaters. Proceedings of the 30th International Conference on Coastal Engineering, ASCE, Vol 5, pp. 4350-4361.

Moody, J.E., 1992. The effective number of parameters: An analysis of generalization and regularization in nonlinear learning systems. In J.E. Moody, S.J. Hanson and R.P. Lippmann (eds.), Advances in Neural Information Processing Systems 4, pp. 847-854. Morgan Kaufmann, San Mateo, California.

Oumeraci, H., Kortenhaus, A. 1999. Probabilistic design tool for Vertical Breakwaters. Final Report, PROVERBS-Proyect. First ed. University of Braunschweig, Germany.

Panizo, A., Briganti, R., 2007. Analysis of Wave Transmission Behind Low-Crested Breakwaters Using Neural Networks, Coastal Engineering, 54(9), 643-656.

Sawaragi, T., Iwata, K., 1979. Irregular wave attenuation due to a vertical breakwater with air chamber. Proceedings of Coastal Structures 1979, ASCE, pp. 29-47.

Seyama, M., Kiyosi, I., 1978.

Proceedings of 25th Coastal Engineering Conference in Japan, pp. 113-117. (in Japanese). Además de incompleta está mal, ni es la XXV congreso ni es 1978… algo anda mal aquí. Si no la fijas bien, elimínala.

Suh, K.D., Park, W.S., 1995. Wave reflection from perforated-wall caisson breakwaters. Coastal Engineering, 26, pp. 177–193.

Suh, K.D., Choi, J.C., Kim, B.H., Park, W.S., Lee, K.S., 2001. Reflection of irregular waves from perforated-wall caisson breakwaters. Coastal Engineering, 44(2), pp. 141–151.

Suh, K.D., Park, J.K., Park, W.S., 2006. Wave reflection from partially perforated-wall caisson breakwaters. Ocean Engineering, 33(2), pp. 264-280.

Tabet-Aoul, E., Lambert, E., 2003. Tentative new formula for maximum horizontal wave forces acting on perforated breakwater caisson. Journal of Waterway, Port, Coastal and Ocean Engineering, 129, pp. 34-40.

Tanimoto, K., Yoshimoto, Y., 1982. Theoretical and experimental study of reflection coefficient for wave dissipating caisson with a permeable front wall. Report of the Port and Harbour Research Institute, 21(3), pp. 44–77 (in Japanese).

Takahashi, S., Tanimoto, K., Shimosako, K., 1994. A proposal of impulsive pressure coefficient for the design of composite breakwaters. Proceedings of the Hydro-Port ’94. Port and Harbour Research Institute, pp. 489–504.

Takahashi, S., Kotake, Y., Fujiwara, R., Isobe, M., 2002. Performance evaluation of perforated-wall caissons by VOF numerical simulations. Proceedings of the 28th International Conference on Coastal Engineering, ASCE, pp. 1365-1376.

Takahashi, S., 2006. Design of vertical breakwaters. Reference Document N34, Port and Harbour Research Institute, Japan.

Teng, B., Zhang, X.T., Ning, D.Z., 2004. Interaction of oblique waves with infinite number of perforated caissons. Ocean Engineering, 31, pp. 615–632.

Twu, S.W., Lin, D.T., 1991. On a highly effective wave absorber. Coastal Engineering, 15, pp. 389–405.

Van Gent, M.R.A., Van den Boogard, H.F.P., 1998. Neural network modelling of forces on vertical structures, Proceedings of the 26th International Conference on Coastal Engineering, ASCE, pp. 2096–2109.

Van Gent, M.R.A., Van den Boogaard, H.F.P., Pozueta, B., Medina, J.R., 2007. Neural network modelling of wave overtopping at coastal structures. Coastal Engineering, 54(8), pp. 586-593.

Verhaeghe, H., De Rouck, J., Van der Meer, J., 2008. Combined classifier–quantifier model: A 2-phase neural model for prediction of wave overtopping at coastal structures. Coastal Engineering, 55(5), pp. 357-374.

Williams, A.N., Mansour, A-E. M., Lee, H.S., 2000. Simplified analytical solutions for wave interaction with absorbing-type caisson breakwaters. Ocean Engineering, 27, pp. 1231-1248.

Yip, T.L., Chwang, A.T., 2000. Perforated wall breakwater with internal horizontal plate. Journal of Engineering Mechanics, 126 (5), pp. 533–538.

Zhu, S.T., Chwang, A.T., 2001. Investigations on the reflection behaviour of a slotted seawall. Coastal Engineering, 43, pp. 93–104.

Zhu, D.T., Zhu, S.W., 2010. Impedance analysis of hydrodynamic behaviours for a perforated-wall caisson breakwater under regular wave orthogonal attack. Coastal Engineering, 57(8), pp. 722-731.

Acronyms

CR	Coefficient of Reflection
ES	Evolutionary Strategy
FN0	Fugazza and Natale (1992) model
FN1	Modified FN0 model
JTB	Jarlan-Type Breakwater
LR	Low Reflectivity
MSE	Mean Squared Error
NN	Neural Network
PSE	Predicted Squared Error
PT	Perforated Typology
PW	Perforated Wall
SA	Simulated Annealing
SW	Slotted Wall
W0	Williams et al. (2000) model
W1	Modified W0 model

Notation

α	Plate orifice coefficient
A_p	Perforated rate of porous wall
A_t	Total rate of porous wall
β	Linear dissipation coefficient
B	Chamber width
C	= 1-PW Relative jet length
Cc	Empirical discharge coefficient of the perforated wall
D(L, B)	Damping function
γ	Constant damping coefficient
g	Acceleration due to gravity
h	Water depth
H	Wave height
H_s	Significant wave height
k	Wave number
i= $\sqrt{-1}$	complex unit
l	Length of the fluid jet flowing through porous wall
L	Wave length of regular wave trains
L_{01}	= m_0/m_1 Mean wave length of random waves
m_k	$=\int_0^\infty f^k S(t)dt$, k-th spectral moment
Nc	Number of chambers
p%	Front wall porosity
P	= lk= Dimensionless jet length

r_{MSE}	$= (MSE)^{1/2}$
R	Energy decay rate
S(f)	Wave spectrum
T	Wave period
T_p	Peak period
ω	Wave angular frequency
W	= tan(kB) = Dimensionless chamber width

Subscript

e	Estimated
o	Observed
FN0	Estimated by FN0 model
FN1	Estimated by FN1 model
W0	Estimated by W0 model
W1	Estimated by W1 model
i	Referring to test i
j	Chamber order

Appendix A. CR estimated by the FN0 model

The coefficient of reflection estimated by the FN0 model, after solving the linearized wave problem given by Fuggazza and Natale (1992) for a single-chamber JTB, is:

$$CR = \frac{\sqrt{(C^2 + W^2)^2 + W^2R^2(W^2R^2 + 2C^2 - 2W^2)}}{C^2 + W^2(1+R)^2} \quad [A.1]$$

in which:

$$R = \beta\left(\frac{k}{\omega}\right) \quad [A.2]$$

$$W = \tan(kB) \quad [A.3]$$

$$C = 1 - PW \quad [A.4]$$

$$P = lk \quad [A.5]$$

where k=2π/L is the wave number; ω=2π/T is the angular frequency, and B= chamber width.

The function β depends on α coefficient, which depends on the empirical discharge coefficient C_C and the geometry of the perforated wall.

$$\beta = \frac{8\alpha}{9\pi} \cdot H \cdot \omega \cdot \frac{W}{\sqrt{W^2(R+1)^2 + C^2}} \cdot \frac{5 + \cosh(2kh)}{2kh + \sinh(2kh)} \quad [A.6]$$

$$\alpha = \left(\frac{1}{pC_c}\right)^2 - 1 \quad [A.7]$$

where H=wave height; h=water depth; p=porosity, and Cc=0.55.

In the case of the double-chamber JTB, a system of 4x2+2 linear equations with the unknown factors (a_0, b_0, c_0, d_0, a_1, b_1, c_1, d_1, a_2, b_2, c_2, and d_2) is obtained:

$$a_0 = \frac{H \cdot g}{2\omega \cosh(kh)} \qquad [A.8]$$

$$b_0 = 0 \qquad [A.9]$$

From the matching conditions at the first and second porous walls between the first and second regions, 2x2 equations are derived:

$$W_0 a_0 + b_0 + W_0 c_0 + d_0 = W_0 a_1 + b_1 + W_0 c_1 + d_1 \qquad [A.10]$$

$$a_0 - W_0 b_0 - c_0 + W_0 d_0 = a_1 - W_0 b_1 - c_1 + W_0 d_1 \qquad [A.11]$$

$$W_1 a_1 + b_1 + W_1 c_1 + d_1 = W_1 a_2 + b_2 + W_1 c_2 + d_2 \qquad [A.12]$$

$$a_1 - W_1 b_1 - c_1 + W_1 d_1 = a_2 - W_1 b_2 - c_2 + W_1 d_2 \qquad [A.13]$$

From the matching conditions of head-loss term at the first and second porous wall, 2x2 equations are derived:

$$\begin{aligned}&\left[P_0 + W_0(1-R_0)\right]a_0 + (1-R_0)b_0 - \left[P_0 + W_0(1+R_0)\right]c_0 - (1+R_0)d_0 = \\ &= W_0 a_1 + b_1 - W_0 c_1 - d_1\end{aligned} \qquad [A.14]$$

$$\begin{aligned}&(1-R_0)a_0 - \left[P_0 + W_0(1-R_0)\right]b_0 - \left[P_0 + W_0(1+R_0)\right]d_0 + (1+R_0)c_0 = \\ &= -W_0 b_1 + a_1 - W_0 d_1 + c_1\end{aligned} \qquad [A.15]$$

$$\begin{aligned}&\left[P_1 + W_1(1-R_1)\right]a_1 + (1-R_1)b_1 - \left[P_1 + W_1(1+R_1)\right]c_1 - (1+R_1)d_1 = \\ &= W_1 a_2 + b_2 - W_1 c_2 - d_2\end{aligned} \qquad [A.16]$$

$$\begin{aligned}&(1-R_1)a_1 - \left[P_1 + W_1(1-R_1)\right]b_1 - \left[P_1 + W_1(1+R_1)\right]d_1 + (1+R_1)c_1 = \\ &= -W_1 b_2 + a_2 - W_1 d_2 + c_2\end{aligned} \qquad [A.17]$$

From the no-flux condition at the solid back wall, 2 equations are obtained:

$$W_2 a_2 + b_2 + W_2 c_2 + d_2 = 0 \qquad [A.18]$$

$$a_2 - W_2 b_2 - c_2 + W_2 d_2 = 0 \qquad \text{[A.19]}$$

The dimensionless parameters W_0, P_0, R_0, W_1, P_1 and R_1 include the distance B_0 and B_1 of the first and second porous wall from the origin, the jet lengths l_0 *and* l_1, and the linear coefficients of dissipation β_0 *and* β_1 at the first and second porous wall:

$$\beta_0 = \frac{8\alpha_0}{9\pi} \cdot U_0 \sinh(kh) \cdot \frac{5 + \cosh(2kh)}{2kh + \sinh(2kh)} \qquad \text{[A.20]}$$

$$\beta_1 = \frac{8\alpha_1}{9\pi} \cdot U_1 \sinh(kh) \cdot \frac{5 + \cosh(2kh)}{2kh + \sinh(2kh)} \qquad \text{[A.21]}$$

where:

$$U_1 = k \cos(kB_1) \cdot \sqrt{\left[d_1 + b_1 - W_1(a_1 + c_1)\right]^2 + \left[a_1 - c_1 - W_1(b_1 + d_1)\right]^2} \qquad \text{[A.22]}$$

$$U_0 = k \cos(kB_0) \cdot \sqrt{\left[d_0 + b_0 - W_0(a_0 + c_0)\right]^2 + \left[a_0 - c_0 - W_0(b_0 + d_0)\right]^2} \qquad \text{[A.23]}$$

And the coefficient of reflection estimated by the FN0 model for a double-chamber JTB is:

$$CR = \frac{\sqrt{c_1^2 + d_1^2}}{a_1} \qquad \text{[A.24]}$$

Appendix B. CR estimated by the W0 model

The governing Laplace equation is modified by adding a damping term for the interior region of the structure:

$$D(L, B) = k^2 \gamma \left(\frac{B}{L} \right) \qquad \text{[B.1]}$$

in which γ is a constant damping coefficient; k is the wave number; B is the chamber width, and L is the wave length.

The reflection coefficient estimated by the W0 model for a single-chamber JTB is:

$$CR = \frac{(kT-1)\alpha_0 \tan\alpha_0 B + ik(1 - S\alpha_0 \tan\alpha_0 B)}{(kT+1)\alpha_0 \tan\alpha_0 B + ik(1 - S\alpha_0 \tan\alpha_0 B)} \quad [B.2]$$

and the reflection coefficient estimated by the W0 model for a double-chamber JTB is:

$$CR = \frac{1 + i[k(S + iT_1) - E]}{-1 + i[k(S + iT_1) - E]} \quad [B.3]$$

where, T represents the inertial effects:

$$T = \frac{8H}{9\pi}\left(p^{-2}Cc^{-2} - 1\right)\frac{\tan(kB)}{\sqrt{\tan(kB)^2(Tk+1)^2 + (1 - Sk\tan(kB))^2}}\frac{5 + \cosh(2kh))}{2kh + \sinh(kh)} \quad [B.4]$$

where H=wave height; p=porosity; h=water depth, and Cc=0.55 is the empirical discharge coefficient.

$$\alpha_0^2 = k^2(1 + i\gamma\frac{B}{L}) \quad [B.5]$$

S represents the resistance, which is usually taken as the barrier thickness; l:

$$S = l \quad [B.6]$$

B1 is the width of the first chamber, and B2 is the width of the second chamber.

$$E = \frac{k\ (G - \tan(\varepsilon_0 B_1))}{\varepsilon_0(G\tan(\varepsilon_0 B_1) - 1)} \quad [B.7]$$

and

$$G = \frac{\varepsilon_0 - \beta_0\varepsilon_0(S_2 + iT_2)\tan(\beta_0 B_2)}{\beta_0 \tan(\beta_0 B_2)} \quad [B.8]$$

in which β_0 and ε_0 satisfy:

$$\beta_0^2 = k^2(1 + i\gamma_2 \frac{B_2}{L}) \quad \text{[B.9]}$$

$$\varepsilon_0^2 = k^2(1 + i\gamma_1 \frac{B_1}{L}) \quad \text{[B.10]}$$

while γ_1 and γ_2 are the damping coefficients for the first porous wall and the second porous wall, respectively.